

Resonance width oscillation in the biripple ballistic electron waveguide

Hoshik Lee^{1,2} and L. E. Reichl¹¹The Center for Complex Quantum Systems, The University of Texas at Austin, Austin, Texas 78712, USA²Department of Physics, Temple University, Philadelphia, Pennsylvania 19122, USA

(Received 20 January 2009; revised manuscript received 31 March 2009; published 8 May 2009)

Interference of quasibound states is studied in a ballistic electron-ripple waveguide with two ripple cavities whose distance apart can be varied. This system is the waveguide analog of Dicke's model for two interacting atoms in a radiation field. Dicke's model has resonances whose widths change in an oscillatory manner as the distance between the atoms is varied. Resonances that form in a biripple waveguide behave in a manner that has some similarity to Dicke's system, but also important differences. We numerically investigate the behavior of resonance widths in the waveguide as the distance between the two ripple cavities changes and we find that the resonance widths oscillate with variation in distance, but the coupling does not decrease as it does in Dicke's system. We discuss differences between our waveguide system and other systems showing the analogous of Dicke effect. We also study scattering-matrix pole trajectories and find that they rotate in counter-clockwise direction on a circle in the complex energy plane.

DOI: 10.1103/PhysRevB.79.193305

PACS number(s): 72.10.-d, 42.50.Gy, 73.63.Kv, 73.23.Ad

In 1954, Dicke¹ showed that a collection of N noninteracting atoms coupled to a common radiation field would spontaneously and coherently radiate with a radiation rate that is N^2 times that of a single atom. This type of coherent radiation is called *super-radiance* and occurs because the N atoms coherently radiate their energy N times as fast a single atom. Twenty years after Dicke's work was published, this so-called *Dicke effect* was observed experimentally in optically pumped hydrogen fluoride gas² and a few years later in atomic europium.³

An analogous effect has been observed in solid-state systems. Shahbazyan and Raikh,⁴ in a theoretical paper, proposed the existence of a Dicke effect in the conductance of a tunneling junction with two resonant impurities. In this system, the bound states of each impurity are indirectly coupled to each other through the electron-wave function in the external leads. The analogy to the Dicke effect has also been proposed for several other mesoscopic systems including quantum dots coupled via a common phonon field,^{5,6} and a quantum wire with side-coupled quantum dots.⁷ Scheibner *et al.*⁸ observed the Dicke effect experimentally in the coherent spontaneous radiation from a two-dimensional (2D) array of exciton quantum dots in CdSe/ZnSe using photoluminescence spectroscopy.

In a previous study,⁹ we showed that the analog of the Dicke effect also appears in the electron conductance of a multiripple ballistic-electron waveguide in a GaAs/AlGaAs heterostructure. Conduction resonances occur in the waveguide due to electron quasibound states created by the multiple ripple cavities in the waveguide. We found broadening and narrowing of resonance widths in electron transmission (conductance) as more ripples are added to the waveguide cavity. However, we could not determine how the resonance widths change as the distance between ripple cavities varies, which is one of the key features of the Dicke effect. In this Brief Report, we study the dependence of resonance widths on the distance between the two cavities of a biripple waveguide using the reaction matrix (R-matrix) theory to generate the scattering matrix (S-matrix) for the waveguide and, thereby, the transmission probability. The R-matrix theory

was originally introduced by Wigner and Eisenbud in 1949 (Ref. 10) for the study of nuclear scattering. Recently, the R-matrix theory has been used to study electron transmission in ballistic electron-ripple waveguides.^{9,11-14} This method generates an exact solution of the Schrödinger equation for electrons propagating in the multiripple waveguide.

Let us consider a waveguide system in which two monoripple cavities are connected to each other by a straight waveguide lead whose length is W . The length of each monoripple cavity is W_r and the upper wall of each cavity is described by an analytic function $y=d-a \cos(2\pi x/W_r)$ (see Fig. 1). The outer end of each cavity is connected to a semi-infinite straight lead whose height is $L=(d-a)$. We assume that the waveguide is built in a two-dimensional electron gas (2DEG) made of a GaAs/AlGaAs heterostructure at a very low temperature. We then use the GaAs-effective mass of the electron $m^*=0.061m_e$, where m_e is the free-electron mass. We use the same parameters that we used in Ref. 9, namely, $a=13.846 \text{ \AA}$, $d=47.269 \text{ \AA}$, and $W=300 \text{ \AA}$ (see Fig. 1). With these parameters we create chaotic and regular dynamical structures in the waveguide-phase space that give rise to well-defined quasibound states. The energy $E_1 = \frac{\hbar^2 \pi^2}{2m^* L^2} = 0.5034074 \text{ eV}$ is the threshold energy to open the first propagating mode in the semi-infinite waveguide lead. We use E_1 as the unit of energy through this report. We only consider the incident-electron energies E which allow one propagating mode so that $E_1 \leq E \leq 4E_1$.

Since electrons freely propagate in the flat waveguide lead

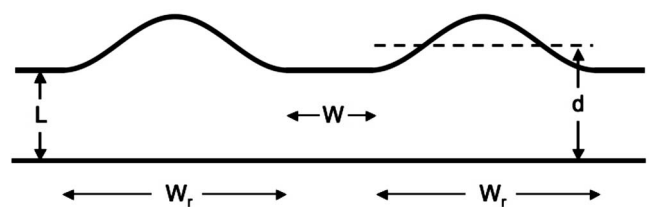


FIG. 1. A biripple waveguide with a flat waveguide between the two ripple cavities.

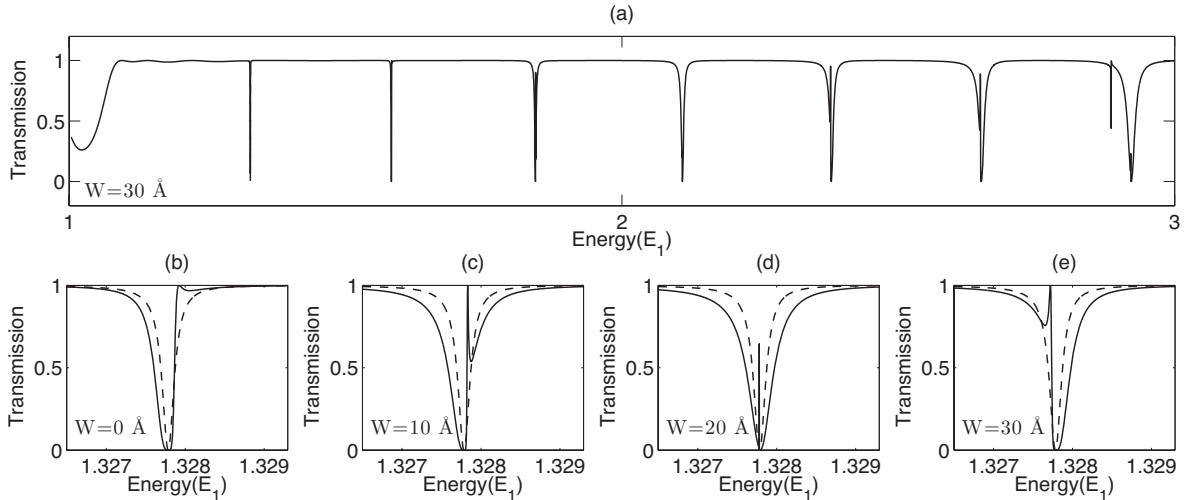


FIG. 2. (a) Electron transmission through the biripple waveguide for distance $W=30$ Å between the two monoripple cavities and for the energy range where only one propagating mode is allowed in the external leads. Also plotted are electron transmission profiles of the lowest-energy resonance in (a) for (b) $W=0$ Å, (c) $W=10$ Å, (d) $W=20$ Å, and (e) $W=30$ Å. As W changes, the width of the resonances and the resonance energies change. The dashed line is the electron transmission for a waveguide with a single monoripple cavity.

that couples the ripple cavities, the electron-wave function acquires the phase $s_W = e^{ik_1 W}$, where $k_1 = \sqrt{(2m^*/\hbar^2)(E - E_1)}$. The S-matrix describing this phase acquisition is a 2×2 diagonal matrix $S_W = \text{diag}(s_W, s_W)$.^{15,16} For a single monoripple cavity connected to leads with only one propagating mode, the S-matrix can be written in the form

$$S_1 = \begin{pmatrix} r_1 & t'_1 \\ t_1 & r'_1 \end{pmatrix}, \quad (1)$$

where $t(t')$ is the transmission-probability amplitude for electrons entering the cavity from the right (left) and $r(r')$ is the reflection-probability amplitude for electrons entering from the right (left). Values for t , t' , r , r' are obtained using the Wigner-Eisenbud method described in Refs. 9 and 11–14. The S-matrix for the second monoripple cavity S_2 can be obtained in the same way. If the two monoripple cavities are identical, S_1 and S_2 are same. We consider only identical ripples in this report. The overall S-matrix S_T is obtained by combining the S-matrices for the two monoripple cavities and the lead that connects them, following the method described in Refs. 15 and 16. We obtain

$$S_T = \begin{pmatrix} r_1 + t'_1 s_W U_2 r_2 s_W t_1 & t'_1 s_W U_2 r'_2 \\ t_2 s_W U_1 t_1 & r'_2 + t_2 s_W U_1 r'_1 s_W t'_2 \end{pmatrix}, \quad (2)$$

where $U_1 = (1 - r'_1 s_W r_2 s_W)^{-1}$ and $U_2 = (1 - r'_2 s_W r_1 s_W)^{-1}$.

Figure 2(a) shows the transmission (conductance) of an electron through the biripple waveguide for $W=30$ Å for a single propagating channel in the waveguide leads. In this interval, there is a sequence of several resonances in the conductance and this broad-scale structure does not change as W is changed. In Figs. 2(b)–2(e), we show the structure of the resonance at $E \approx 1.328E_1$ for $W=0, 10, 20,$ and 30 Å. The dashed line in each figure is the electron transmission for a waveguide with a single monoripple cavity. We can see the resonance width narrowing and broadening (Dicke effect) as W is increased.

Figure 3(a) shows how the S-matrix poles for the quasi-bound states that give rise to these resonances change position in the complex energy plane. The eight-pronged star in the middle of this figure gives the location of the single pole for the monoripple waveguide that gives the dashed line in Fig. 2. In the biripple waveguide, two poles (phase shifted by π) move in a circle around the monoripple pole as W increases. These two poles induce two resonance shapes in the transmission plots (Fig. 2), a broad one and a very narrow one. The behavior of the two poles indicates that not only the widths but also the resonance energy (real part of the pole) changes with W . As W increases, one of the poles gets closer to the real axis while the other moves away from the real axis [see Fig. 3(a)]. As one of the poles gets closer to the real axis, its corresponding resonance becomes sharper (long-lived state, *subradiance*) while the other resonance becomes broader (short-lived state, *super-radiance*). The corresponding narrowing and broadening of the resonance widths is shown in Fig. 2. We have also inserted in this figure spatial plots of the scattering state (real part only) associated with each of these poles. For the values of W shown in Fig. 3(a), the pole close to the real axis (long-lived quasibound state) is antisymmetric and the pole far from the real axis (short-lived quasibound state) is symmetric. For example, the symmetric quasibound state for $W=20$ Å corresponds to Dicke's “super-radiant” state and decays twice as fast as the corresponding quasibound state associated with a single monoripple waveguide (the eight-pronged pole). The antisymmetric state for $W=20$ Å corresponds to a “subradiant” state and lives twice as long as the quasibound state in the monoripple waveguide. If there was one electron in each monoripple cavity, the super-radiant state would emit an electron-current pulse that is $2^2=4$ times (two electrons twice as fast) that for a single electron in a monoripple waveguide.

As the poles rotate, it becomes possible for one of the poles to reach the real axis and then the width of the reso-

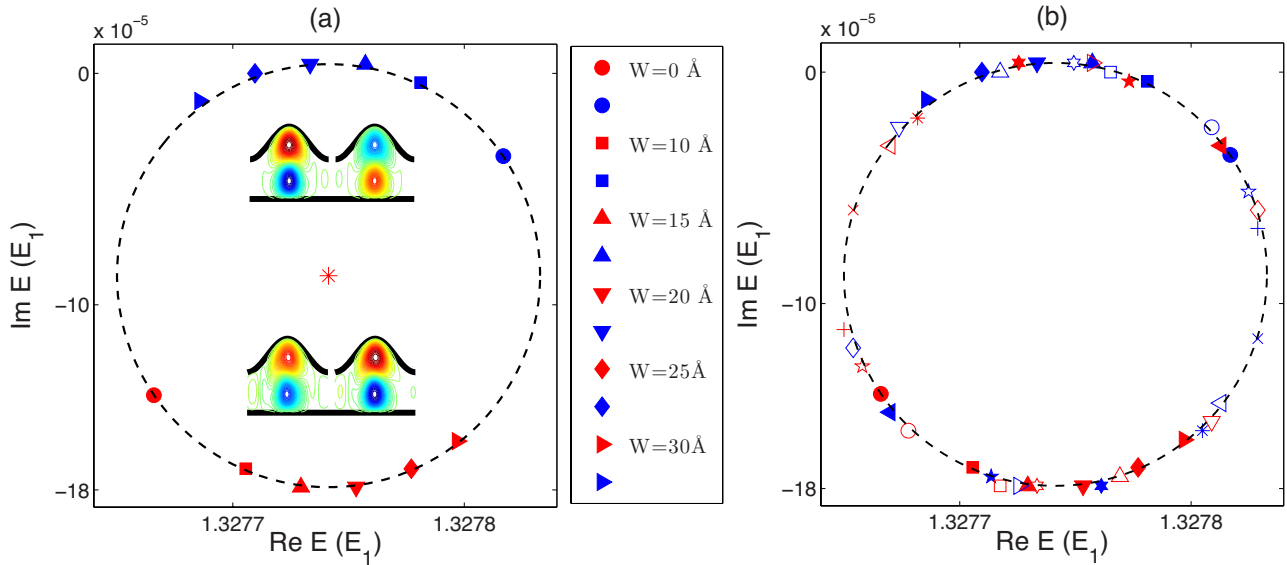


FIG. 3. (Color online) (a) S-matrix poles for the biripple waveguide with different values of W . Each pole rotates on a circle [whose center is the S-matrix pole of the waveguide (red *) with a single cavity] in counterclockwise direction as W increases. The pair of poles has π -phase difference so that they are located in the opposite direction on the circle. Upper (lower) inset: The spatial plots of the real part of the scattering states for $E=1.32776E_1$ ($E=1.32783E_1$) when $W=25$ Å. (b) S-matrix pole trajectories for biripple waveguide as W varies from 0 Å to 250 Å.

nance collapses, indicating that the lifetime of the resonance has become infinite. When this happens the resonance state is completely decoupled from external leads. This phenomenon has been called “bound state in continuum” (BIC) in other studies.^{17,18} This effect might allow controlled storage and release of electrons in such devices.

Because the poles rotate in a circle, it is possible and useful to write analytic expressions for the pole positions in the complex energy plane. The S-matrix pole position for a waveguide with a single monoripple cavity can be written $E_{\text{mon}}=E_0-i\Gamma_0$. Since S-matrix poles for the biripple waveguide rotate on a circle around this pole, their positions can be written as a sinusoidal function of W such that $E_{\text{sup}}=E_+-i\Gamma_+$ ($E_{\text{sub}}=E_- -i\Gamma_-$) denotes the position of the super-radiant (subradiant) pole, where

$$E_+ = E_0 + \Gamma_0 \sin(k_1 W + \delta_0), \quad E_- = E_0 - \Gamma_0 \sin(k_1 W + \delta_0), \quad (3)$$

and

$$\Gamma_+ = \Gamma_0(1 + \alpha), \quad \Gamma_- = \Gamma_0(1 - \alpha). \quad (4)$$

In Eqs. (3) and (4), $\alpha = \cos(k_1 W + \delta_0)$ is a measure of the coupling between the cavities, k_1 is a wave number at a resonance energy, and a phase factor δ_0 is used because a pole is not on the real axis when $W=0$. Figure 3(b) shows the pole trajectories in the complex energy plane as W increases up to 250 Å. It confirms that the pair of poles always stays on a circle and it verifies Eq. (3) and (4).

As was shown in Refs. 9 and 14, a sequence of resonances occur as energy in the interval $E_1 \leq E \leq 4E_1$ is increased. Figures 4(a) and 4(b) show the widths of resonances at energies $E=1.3278E_1$ and $E=1.5830E_1$, respectively, as a function of the distance W . The resonance widths are clearly

sinusoidal functions of W , which indicates that the coupling between the two cavities varies sinusoidally with increasing W . Figure 4(b) oscillates slightly faster than Fig. 4(a) because of its higher-resonance energy. In Eq. (4), the coupling parameter $\alpha = \cos(k_1 W + \delta_0)$ is a sinusoidal function which gives the oscillatory behavior of the widths in Fig. 4. This behavior of the coupling parameter in our one-dimensional (1D) system is different from that seen in higher dimension. In Ref. 4, the coupling between a collective state of two impurities and external electron-wave function (a 2D system) is a Bessel function [$J_0(s_{12}/\lambda_f)$] (see Eq. 19 in Ref. 4). In the

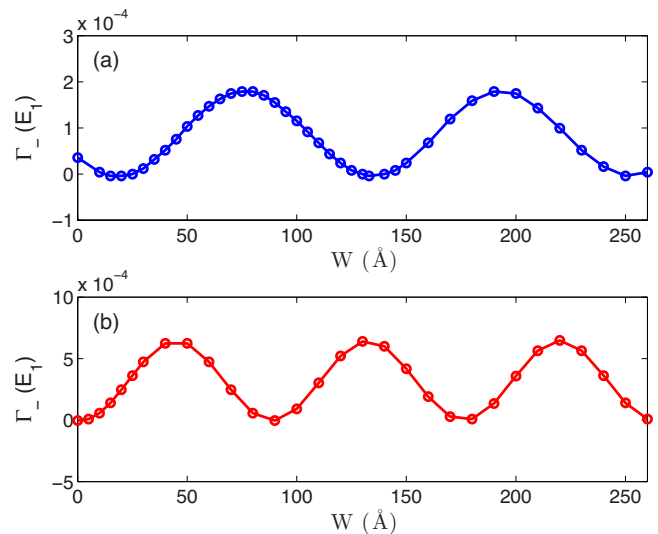


FIG. 4. (Color online) The resonance width Γ_- for a biripple waveguide. Γ_- oscillates as W is varied. The blue line (a) is for the resonance near $E=1.3278E_1$. The red line (b) is for the resonance near $E=1.5830E_1$.

double quantum dots coupled through the common phonon fields¹⁹ [a three-dimensional (3D) system], the coupling parameter is a zeroth-order spherical Bessel function [$\sin(Qd)/Qd$]. In these 2D and 3D systems, the coupling parameter decays with the distance between two atoms, as is the case for the Dicke system (a 3D system). This dependence of the coupling on zeroth-order Bessel functions (which have their largest values at long wavelength) means that in 2D and 3D systems, the super-radiance occurs predominantly with the wavelengths much longer than the atomic distance. However, in our 1D waveguide system (the transverse direction is constrained), the coupling parameter α does not decay. Therefore, the super-radiant resonance exists regardless of the wavelength of the electron. It is possible that a super-radiant resonance appears with a very large distance between two cavities but it could not exceed the coherence length of electrons in the waveguide. In 2DEGs made of GaAs/AlGaAs, for example, at a very low temperature, the coherence length is about 10 μm .

As we have seen in Figs. 2 and 3, there are two S-matrix poles associated with each resonance in the electron transmission. The behavior of these two poles is associated with the symmetry of the scattering wave function at resonance energies. In Dicke's model, subradiant resonance is related to the antisymmetric collective state of the atomic system and the super-radiant resonance is related to the symmetric collective state. In the biripple waveguide, as the pair of poles rotate in a counterclockwise direction (with increasing distance between the two ripple cavities), they each maintain the symmetry of their corresponding resonance wave function. The antisymmetric state is super-radiant when $\alpha < 0$ and the symmetric state is super-radiant when $\alpha > 0$. Therefore, super-radiant resonances appear in a sinusoidal manner as W increases and the symmetry of their corresponding scat-

tering wave functions alternates between symmetric and antisymmetric with increasing W .

In conclusion, we have studied the behavior of quasi-bound states in a biripple waveguide as the distance between the two ripple cavities changes. We found that the widths and positions of the resonances associated with the quasibound-state poles change in a sinusoidal way with variation in the distance between the ripple cavities. In 2D and 3D models of the Dicke effect, the coupling parameter decays when the distance between two atoms (impurities or quantum dots) is longer than the wavelength of photon or electron. In the ripple waveguide system, the coupling parameter does not decay because the waveguide is a quasi-1D system. We also studied the trajectories of S-matrix poles in the complex energy plane. We found that the pair of poles that give rise to the super- and subradiant resonances in the electron transmission, rotate on a circle centered on the S-matrix pole for the waveguide with a single cavity and are phase-shifted by π . Therefore, super-radiant and subradiant resonances appear in oscillatory manner as the distance between cavities is changed. Furthermore, as the S-matrix poles rotate, the symmetry of the electron state associated with the super-radiant (subradiant) resonance alternates between symmetric and antisymmetric with increasing distance between the two ripple cavities. We believe that an experimentalist may be able to observe the broadening and shortening of widths even if two cavities are not identical as long as the resonance energies are close to each other.

The authors wish to thank the Robert A. Welch Foundation (Grant No. F-1051) for support of this work. We also thank to Kyungsun Na for her advice and useful discussions and we thank the Texas Advanced Computing Center (TACC) for use of their facilities.

¹R. H. Dicke, Phys. Rev. **93**, 99 (1954).

²N. Skribanowitz, I. Herman, J. MacGillivray, and M. Feld, Phys. Rev. Lett. **30**, 309 (1973).

³Ph. Cahuzac, H. Sontag, and P. E. Toschek, Opt. Commun. **31**, 37 (1979).

⁴T. V. Shahbazyan and M. E. Raikh, Phys. Rev. B **49**, 17123 (1994).

⁵T. Vorrath and T. Brandes, Phys. Rev. B **68**, 035309 (2003).

⁶V. V. Temnov and U. Woggon, Phys. Rev. Lett. **95**, 243602 (2005).

⁷P. Orellana, F. Dominguez-Adame, and E. Diez, Physica E (Amsterdam) **35**, 126 (2006).

⁸M. Scheibner, T. Schmidt, L. Worschech, A. Forchel, G. Bacher, T. Passow, and D. Hommel, Nature Phys. **3**, 106 (2007).

⁹H. Lee and L. E. Reichl, Phys. Rev. B **77**, 205318 (2008).

¹⁰E. P. Wigner and L. E. Eisenbud, Phys. Rev. **72**, 29 (1947).

¹¹L. E. Reichl, *The Transition to Chaos*, 2nd ed. (Springer, New York, 2004), Chap. 7.

¹²G. Akguc and L. E. Reichl, Phys. Rev. E **64**, 056221 (2001).

¹³G. B. Akguc and L. E. Reichl, Phys. Rev. E **67**, 046202 (2003).

¹⁴H. Lee, C. Jung, and L. E. Reichl, Phys. Rev. B **73**, 195315 (2006).

¹⁵T. S. Chu and T. Itoh, IEEE Trans. Microwave Theory Tech. **34**, 280 (1986).

¹⁶S. Datta, M. Cahay, and M. McLennan, Phys. Rev. B **36**, 5655 (1987).

¹⁷G. Ordóñez, K. Na, and S. Kim, Phys. Rev. A **73**, 022113 (2006).

¹⁸G. Cattapan and P. Lotti, Eur. Phys. J. B **66**, 517 (2008).

¹⁹T. Brandes and B. Kramer, Phys. Rev. Lett. **83**, 3021 (1999).